PHYSICAL REVIEW B, VOLUME 64, 201317(R)

Extreme magnetic modulation of the exciton transfer rate between unequal quantum wells

S. K. Lyo
Sandia National Laboratories, Albuquerque, New Mexico 87185

(Received 6 April 2001; revised manuscript received 31 July 2001; published 5 November 2001)

We show that a moderate in-plane magnetic field quenches the Stokes transfer of excitons between direct and indirect (i.e., type II) quantum wells at low temperatures. The transfer is due to the decay of an exciton in the initial well into a free electron-hole pair in the final well. Higher fields open, within a narrow range of field, a new dramatically enhanced resonant transfer channel for both the Stokes and the anti-Stokes transfer between the higher-energy direct and lower-energy indirect exciton states. The rates are calculated for $GaAs/Al_xGa_{1-x}As$ quantum wells.

DOI: 10.1103/PhysRevB.64.201317 PACS number(s): 71.35.Ji, 78.55.Cr, 78.66.Fd

Energy transfer of excitons in quasi-two-dimensional semiconductor quantum-wells (QWs) plays an important role in optoelectronic devices. While intra-QW exciton transfer has been studied extensively,[1] interwell transfer has received less attention.[2–4] Proposed mechanisms for the transfer between $GaAs/Al_xGa_{1-x}As$ double QWs include dipole-dipole[2,4] and photon-exchange[4] mechanisms as well as carrier tunneling through GaAs clusters in the barrier.[3] Recent data[2,3] indicate that the transfer is efficient over a long range as predicted by the photon-exchange mechanism. We show that a moderate in-plane magnetic field (B) quenches the $B=0$ Stokes rate between direct and indirect quantum wells at low temperatures. Higher fields induce, within a narrow range of B, a new dramatically enhanced resonant rate between the higher-energy direct and lower-energy indirect exciton states. The B-induced enhancement over the $B=0$ rate is a few orders of magnitude. We find that the dipolar and photon-exchange interactions yield very different B-dependent rates. Especially, the photon-exchange transfer rate is turned on and off by B very sharply compared to that of the dipolar rate, due to its sharp cutoff for a large momentum exchange.

The exciton transfer under investigation occurs between two wells QW1 and QW2 illustrated in Fig. 1, where QWs are GaAs and barriers are $Al_xGa_{1-x}As$. QW1 is direct. QW2 consists of double QWs and is transformed into an indirect (i.e., type II) QW by applying a large electric field E, which produces the slanted structure in Fig. 1. Spatially indirect excitons have been observed from such structures with $E>10$ kV/cm.[5–7] In Fig. 1 the two QWs in QW2 are narrower than QW1, yielding a much greater direct electron-hole (e-h) energy separation in QW2 than in QW1 and thus a negligible rate from QW1 to the direct excitons in QW2.

Transfer of an exciton with a center-of-mass (CM) wave number K takes place through the interaction $\mathcal{J}(K)$ which demotes the electron into the hole in QW1 while promoting a valence electron into the indirect conduction band in QW2. The dominant coupling is via dipole-dipole and photon-exchange interactions. The magnitude of $\mathcal{J}(K)$ decreases rapidly for large K. The dipolar rate decays as d^{-4} and is dominant only when the transfer distance d (in Fig. 1) is short (e.g., $d \lesssim 80$ Å).[4] On the other hand, the photon-exchange rate has a long range (i.e., logarithmic) dependence and is dominant at a large d considered here.

The Hamiltonian of an electron and a hole in QW1 or separately in QW2 in Fig. 1 is given by $H=H_K+V(z)+V_{eh}$, where H_K is the kinetic energy, $V(z)$ is the single-QW (double-QW) confinement energy for QW1 (QW2), and V_{eh} is the Coulomb interaction energy. Assuming that $\mathbf{B}\|\mathbf{x}$, using a vector potential $\mathbf{A}=(0,-Bz,0)$, H_K is given by[8]

$$H_K=\frac{\hbar^2}{2M}\left[K_x^2+\left(K_y-\frac{z_e-z_h}{\ell^2}\right)^2\right]+\frac{\hbar^2}{2\mu}\left[-\frac{\partial^2}{\partial x^2}+\left(\frac{1}{i}\frac{\partial}{\partial y}-\frac{\alpha_h z_e+\alpha_e z_h}{\ell^2}\right)^2\right]-\left(\frac{\hbar^2}{2m_e^*}\frac{\partial^2}{\partial z_e^2}+\frac{\hbar^2}{2m_{zh}^*}\frac{\partial^2}{\partial z_h^2}\right), \quad (1)$$

where $\ell=\sqrt{\hbar c/eB}$, $M=m_e^*+m_h^*$ is the total in-plane mass, μ is the reduced mass, $\mathbf{K}$ is the CM wave vector, $\alpha_{e,h}=m_{e,h}^*/M$, and x,y are the relative coordinates. The electron mass m_e^* is assumed to be isotropic. The potential energy V is independent of B. The wave number $K_y=k_{cy}-k_{vy}$ in Eq. (1) is displaced by $(z_e-z_h)/\ell^2$ owing to the fact that the vector potential displaces the wave number k_{cy} (k_{vy}) of the electron in the conduction (valence) band by z_e/ℓ^2 (z_h/ℓ^2).[8] We now employ a quasi-two-dimensional approximation. The quantity $d_{eh}=z_e-z_h$ is large only for the indirect exciton in QW2 and is neglected for the direct exciton in QW1. This kind of indirect excitons in both real and k space have been observed recently.[5] The rest of the B-dependent quantity, $\delta k_B\equiv(\alpha_h z_e+\alpha_e z_h)/\ell^2$ in Eq. (1) changes only the phase of the wave function for the relative motion in this approximation and can be neglected. In the three-dimensional limit, however, the magnetic field not only deforms the wave function but also enhances the oscillator strength.[9]

The energy dispersion curve for the CM motion in the y direction in QW2 is then displaced by $\delta K\equiv d_{eh}/\ell^2\propto B$ relative to that of QW1 as shown in Figs. 2. Here, d_{eh} is the e-h separation in the z direction in QW2. In Fig. 2(a), the dominant Stokes transfer mechanism of an exciton from QW1 to QW2 at $B=0$ is through decay into a free indirect e-h pair in QW2.[2,4] This is explained in the following way. The CM energy is conserved through the transfer process due to the $\mathbf{K}$ conservation. The extra energy can be relaxed either through phonon emission or through splitting the exciton into a free e-h pair, thereby dissipating the energy into the kinetic energy of the relative e-h motion. These e-h pairs form excitons in a time scale ($\sim$ps) much shorter than the transfer

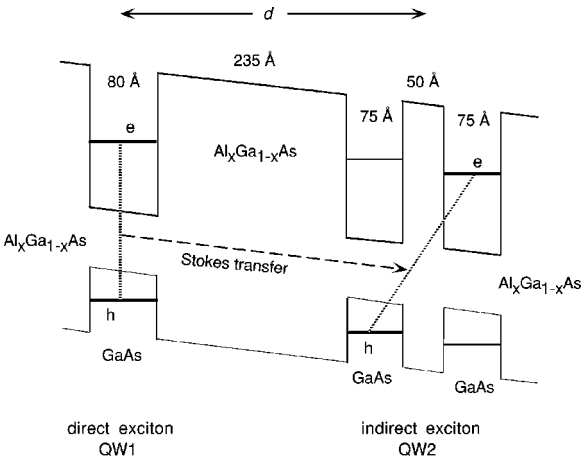

FIG. 1. The exciton transfer occurs between a direct QW (QW1) and an indirect QW (QW2). The *e-h* separation in QW2 is achieved by a large DC electric field as shown. The shaded lines connecting the *e-h* pair designate exciton binding.

time. The phonon-assisted rate was shown to be small.[4] For $B>0$, simultaneous energy and momentum conservation is satisfied at the black dot in Fig. 2(b), opening a fast resonant channel. This transfer is most efficient when the resonant K_y lies within the thermal range of the initial exciton. Also, the coupling energy $\mathcal{J}(K)$ becomes very small for large K as will be shown later. Therefore, the resonant rate is large only within a narrow range of B. Note also that the transfer through the *e-h* decay is possible only for the initial K_y states to the right of the black dot, yielding a negligible rate for large B. The resonant rate is negligible when the indirect QW2 has a higher energy than QW1 because the magnitude of the resonant K_y is always large.

Figures 3 illustrate the mechanism of the anti-Stokes transfer. At $B=0$ in Fig. 3(a), the transfer occurs through second-order phonon-absorption processes in contrast with the first-order process considered here. Using an earlier theory,[4] we find that the phonon-assisted processes and the two-exciton Auger process[4] yield negligible rates for both the Stokes and the anti-Stokes transfer. Moderate magnetic fields open two channels as illustrated in Figs. 3(b) and 3(c) by displacing the two curves relative to each other and making them intersect. For the anti-Stokes transfer from a direct to an indirect QW, the $|K_y|$ value of the intersecting point is large as seen from Fig. 3(b), yielding negligible coupling $\mathcal{J}(K)$. This is not true for the anti-Stokes transfer from an indirect to a direct QW in Fig. 3(c), yielding a large coupling $\mathcal{J}(K)$ and thereby a large transfer rate at optimum fields.

The transfer rate of an exciton from QW1 to QW2 through decay into a free *e-h* pair is given for the processes illustrated in Fig. 2 by

$$W_\alpha^{eh}=\frac{2\pi}{\hbar}\left\langle \mathcal{J}_\alpha^{eh}(K)^2\sum_{\mathbf{k}}\ \delta\left(\left\{\frac{\hbar^2}{2M}(K_y-\delta K)^2+\frac{\hbar^2}{2\mu}k^2-\Delta\right\}-\left\{\frac{\hbar^2}{2M}K_y^2-E_{1B}\right\}\right)\right\rangle_T, \tag{2}$$

where the subscript $\alpha=dp,\ ph$ denotes the dipole-dipole and photon-exchange interaction, respectively, $\delta(x)$ is the delta function, the symbol $\langle\cdots\rangle_T$ signifies the Boltzmann average with respect to the initial state $\mathbf{K}$, Δ is the energy-gap difference between QW1 and QW2, and $\mathbf{k}$ is the wave vector for the relative motion of the free *e-h* pair in QW2. The quantity E_{jB} is the exciton binding energy in the jth QW. Equation (2) yields

$$W_\alpha^{eh}=\frac{2S\mu}{\pi\hbar^3}\int_0^\infty dx\int_{y^*}^\infty dy\, e^{-(x^2+y^2)}\mathcal{J}_\alpha^{eh}(K)^2, \tag{3}$$

where S is the area of the QWs, $(x,y)=\xi_T\mathbf{K}$, $\xi_T=\sqrt{\hbar^2\beta/2M}$, $\beta=1/k_BT$, and $y^*=\xi_TK_y^*$. Here $K_y^*=[\delta K-2M(\Delta-E_{1B})/\hbar^2\delta K]/2$ is the lower limit of the K_y integration. This limit indicates that the *e-h* decay is energetically possible only for the K_y states to the right side of the black dot in Fig. 2 where the energy of QW1 is greater than that of QW2 at the same $\mathbf{K}$. The lower limit K_y^* sweeps from $K_y^*=-\infty$ to $K_y^*=+\infty$ as B increases from $B=0$ to $B=\infty$ for $\Delta-E_{1B}>0$, decreasing W_α^{eh} monotonically.

Direct resonant transfer occurs through the black-dot state in Fig. 2(b). Here both the initial and final states are exciton

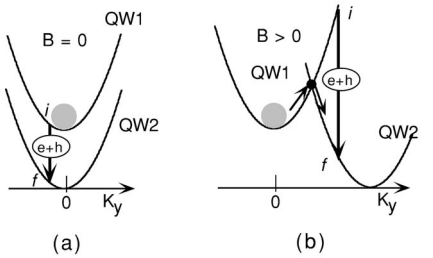

FIG. 2. Stokes transfer mechanisms (shown by the arrows). The energy dispersion curves for the center-of-mass motion in the transverse (i.e., y) direction in QW1 and QW2 are displaced relative to each other by the magnetic field B. (a) The Stokes transfer occurs at $B=0$ through decay into a free *e-h* pair. (b) For $B>0$, additional fast resonant tunneling is possible from QW1 to QW2 through the resonant state denoted by the black dot. The phase space for the decay into an *e-h* pair is reduced.

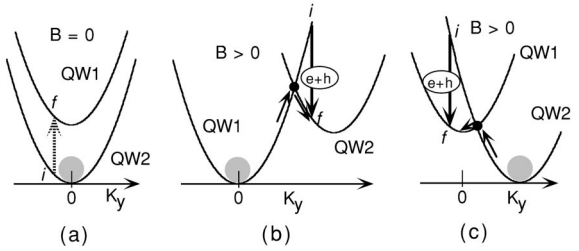

FIG. 3. Anti-Stokes transfer mechanisms (shown by the arrows). The energy dispersion curves for the center-of-mass motion in the transverse (i.e., y) direction in QW1 and QW2 are displaced relative to each other by the magnetic field B. (a) Direct resonant energy transfer or transfer of an exciton through decay into an *e-h* pair is impossible at $B=0$. (b) Transfer mechanisms from the direct QW1 to the indirect QW2 for $B>0$. (c) Transfer mechanisms from the indirect QW2 to the direct QW1 for $B>0$

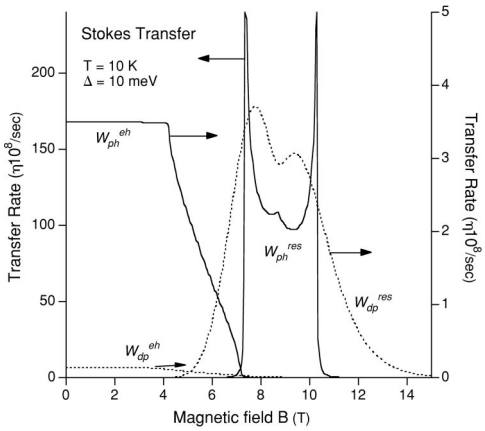

FIG. 4. The Stokes transfer rate from direct QW1 to indirect QW2 via photon-exchange (solid curves) and dipole-dipole (dotted curves) interactions. The curves with peaks in the range $B=7-11$ T are from the resonant transfer, while those that decay beyond $B=5$ T are from the creation of an e-h pair. The sample parameters are given in Table I and η is defined in the text.

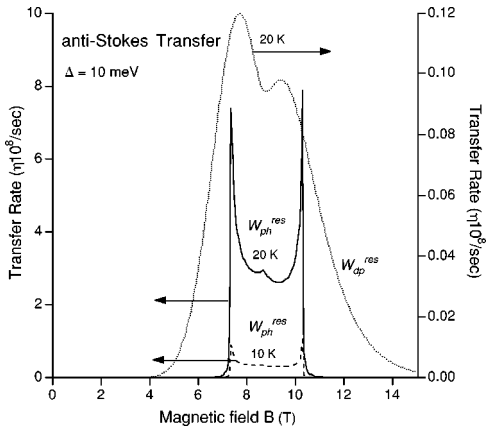

FIG. 5. The anti-Stokes resonant transfer rate from indirect QW2 to direct QW1 via photon-exchange (solid and dashed curves) and dipole-dipole (dotted curve) interactions. The dipolar rate at 10 K is much smaller than that at 20 K and is not shown. Sample parameters are given in Table I and η is defined in the text.

states. The rate is given by Eq. (2) with the following changes. The initial energy is given by the second curly brackets in the delta function in Eq. (2) and the final energy by the first brackets with $\hbar^2/2\mu k^2$ replaced by $-E_{2B}$. The coordinate k is irrelevant and omitted. We find after the Boltzmann average

$$W_\alpha^{\rm res}=\frac{2\beta}{\hbar\,\delta K\xi_T}\int_0^\infty d\,x\,e^{-(x^2+y^{*2})}\mathcal{J}_\alpha^{\rm res}(K)^2, \qquad (4)$$

where $x=\xi_T K_x$, $y^*=\xi_T K_y^*$, $K=\sqrt{K_x^2+K_y^{*2}}$ and $K_y^*=[\,\delta K-2M(\Delta-E_{1B}+E_{2B})/\hbar^2\delta K]/2$. The quantity K_y^* sweeps from $K_y^*=-\infty$ to $K_y^*=+\infty$ as B increases from $B=0$ to $B=\infty$ for $\Delta-E_{1B}+E_{2B}>0$. In this case, the resonant rate becomes extremely large within a narrow range of B when $|K_y^*|$ lies within the thermal range around $K_y=0$ as will be seen later.

Stokes transfer from an indirect to a direct QW can be treated in a similar way. In this case, QW1 and QW2 are switched in Figs. 2 and the upper parabola moves to the right as B increases. The rate W_α^{eh} has a qualitatively similar B dependence. In contrast, the resonant transfer rate $W_\alpha^{\rm res}$ is negligibly small in this case, because $K_y^*=[\,\delta K+2M(\Delta+E_{1B}-E_{2B})/\hbar^2\delta K]/2$ has a minimum at $K_y^*=\sqrt{2M(\Delta+E_{1B}-E_{2B})/\hbar^2}$ and is large for all B, not only yielding small $\mathcal{J}(K)$ but also requiring a large activation energy.

In the following, we evaluate $\mathcal{J}_\alpha^{eh}(K)$ and $\mathcal{J}_\alpha^{\rm res}(K)$ for dipole-dipole and photon-exchange interactions. Specific expressions for these interactions have been obtained earlier by the author, for transfer between direct QWs.[4] An extension of these results to the transition between a direct and indirect QW is straightforward. For the decay of an exciton into an e-h pair through dipolar interaction, we find in a quasi-two-dimensional approximation:[4]

$$\mathcal{J}_{dp}^{eh}(K)=\mathcal{J}_0^{eh}[\cos(2\phi_{\mathbf{K}}-\phi_D)+\cos\phi_D]Ke^{-Kd}, \qquad (5)$$

where $\mathcal{J}_0^{eh}=2\sqrt{2\pi}D_1D_2e^2\langle\psi_h|\psi_e\rangle/(\kappa a_B\sqrt{S})$, κ is the bulk dielectric constant, a_B is the bulk Bohr radius in the QW material, and d is the distance from the center of QW1 to the position of the peak of the product of the electron and hole confinement wave functions ψ_e and ψ_h in QW2. The quantity $\phi_{\mathbf{K}}$ in Eq. (5) is the angle between the initial transition dipole moment $\mathbf{D}_1$ in a unit cell in QW1 and $\mathbf{K}$. ϕ_D is the angle between $\mathbf{D}_1$ and the final transition diploe moment $\mathbf{D}_2$ in QW2. These moments are from the heavy-hole state due to the QW confinement and are assumed to be in the QW plane, following the treatments in Refs. 2 and 4. Summing over two equal contributions from $\mathbf{D}_2\|,\perp\mathbf{D}_1$, we find

$$\mathcal{J}_{dp}^{eh}(K)^2=2\mathcal{J}_0^{eh\,2}K^2e^{-2Kd}, \qquad (6)$$

where a cross term linear in K_xK_y is dropped because it cancels out from the K_x integration in Eqs. (3) and (4) due to the odd parity. Similarly we find

$$\mathcal{J}_{dp}^{\rm res}(K)^2=2\mathcal{J}_0^{\rm res2}K^2e^{-2Kd}. \qquad (7)$$

TABLE I. Sample parameters for GaAs/Al_xGa_{1-x}As employed in the text.[4]

Electron mass m_e^*	$0.067m_0$	Dielectric constant κ	12.4
Hole mass m_h^*	$0.14m_0$	Dipole moment $D_1=D_2$	5.5 Å
Band gap E_g	1.52 eV	Refractive index n	3.68
Energy mismatch Δ	10.0 meV	Direct exciton binding energy[10] E_{1B}	8.0 meV
Electron-hole separation d_{eh}	125.0 Å	Indirect exciton binding energy[5] E_{2B}	3.0 meV
QW1-QW2 separation d	375.0 Å	Exciton damping Γ	0.1 meV

The coupling $\mathcal{J}_0^{\rm res}=8D_1D_2e^2\langle\psi_h|\psi_e\rangle/(\kappa a_B^2)$ for the resonant exciton-to-exciton transfer has a slightly different form from $\mathcal{J}_0^{eh}$ because of the different final-state wave function.

The square of the effective photon-exchange interaction for the decay of an exciton in QW1 into a free *e-h* pair in QW2 is given after summing over $\mathbf{D}_2\|,\perp\mathbf{D}_1$ and dropping a linear term in K_xK_y by[4]

$$\mathcal{J}_{ph}^{eh}(K)^2=\mathcal{J}_{\rm rad}^{eh\,2}[|I_0(Kd)|^2+|I_1(Kd)|^2], \tag{8}$$

where $\mathcal{J}_{\rm rad}^{eh}=4\sqrt{2}E_ge^2D_1D_2/(\hbar\sqrt{\pi S}\,{\rm c\,n}\,a_B)$, E_g is the gap energy in the well, c,n the speed of light and the refractive index, and

$$I_\nu(x)=\int_0^\infty dz\frac{z^{2\nu}\cos z}{[x^2+z^2]^\nu}\left\{\frac{1}{\sqrt{x^2+z^2}}+\frac{1}{d/\xi_g-\sqrt{x^2+z^2}-i\gamma}\right\}, \tag{9}$$

where $\gamma=\Gamma d/E_g\xi_g\ll 1$, $\xi_g=\hbar{\rm c}/{\rm n}E_g$, and Γ is the exciton damping. For resonant exciton-to-exciton tunneling we find

$$\mathcal{J}_{ph}^{\rm res}(K)^2=\mathcal{J}_{\rm rad}^{\rm res2}[|I_0(Kd)|^2+|I_1(Kd)|^2], \tag{10}$$

where $\mathcal{J}_{\rm rad}^{\rm res}=16E_ge^2D_1D_2/(\pi\hbar\,{\rm c\,n}\,a_B^2)$. The difference of the latter expression from $\mathcal{J}_{\rm rad}^{eh}$ is due to different final wave functions.[4]

In Fig. 4 we display the Stokes transfer rates from QW1 to QW2. The rates are calculated from Eqs. (3) and (4) for the *e-h* creation mechanism (W_α^{eh}) and the resonant mechanism ($W_\alpha^{\rm res}$) using photon-exchange ($\alpha=ph$, solid curves) and dipole-dipole ($\alpha=dp$, dotted curves) interactions. The resonant transfer yields an extreme enhancement of the rate in the range $B=7-11$ T compared to the rate from the *e-h* creation mechanism for both the photon-exchange and dipolar interactions. The sample parameters are given in Table I and $\eta=|\int\psi(z,z)dz|^2\simeq\langle\psi_h|\psi_e\rangle^2(\simeq 10^{-4}-10^{-3})$ for the vertical axis.[4,5,10] Here $\psi(z_e,z_h)$ is the *z*-component of the indirect exciton wave function in the quasi-2D approximation and $\psi_e(z)$ ($\psi_h(z)$) the free electron (hole) wave function. In Table I, $\Delta=10$ meV corresponds to $E=5$ kV/cm in Fig. 1. Calculating the accurate binding energies is beyond the scope of this paper. Their role here is to determine the effective energy mismatch $\Delta_{\rm eff}=\Delta-\eta_1(E_{1B}-\eta_2E_{2B})$, $\eta_1=\pm 1,\eta_2=1,\ 0$ for various transitions. Therefore, rough numbers estimated from Refs. 5 and 10 are used for E_{1B} and E_{2B}. The quantity $\Delta_{\rm eff}$ and therefore E_{1B},E_{2B} can be determined from the data using the sharp turn-on and turn-off fields to be discussed below. Also, a numerical value of m_{zh}^h is not necessary in this approach. The sharpness of the peaks of the solid curve near $B=7.3$ T and $B=10.3$ T in Fig. 4 depends logarithmically on Γ. The rates decrease for increasing *T* due to the fact that a larger CM thermal energy, namely a larger *K*, decreases $\mathcal{J}(K)$. The rates in Fig. 4 are reduced by about 30%–40% when *T* is increased from 10 K to 20 K, while their *B*-dependence remain about the same. For larger Δ, the *B* dependences of the rates are similar but the scale of *B* is expanded. This is anticipated from the fact that the crossing of the two dispersion curves occurs at $K_y^*=[\delta K-2M(\Delta-E_{1B}+\xi E_{2B})/\hbar^2\delta K]/2$, where $\delta K\propto B$, $\xi=0$ for W_{ph}^{eh}, and $\xi=1$ for $W_{ph}^{\rm res}$. It is seen from this relationship and Fig. 2(b) that a large *B* is required for the black dot to sweep across the thermal range near $K_y^*=0$. The enhanced rate $W_{ph}^{\rm res}$ emerges on the right side of the tail of W_{ph}^{eh} in Fig. 4 because of the binding energy E_{2B} of the indirect exciton in QW2.

Figure 5 displays the resonant anti-Stokes transfer rate from QW2 to QW1 illustrated in Fig. 3(c). The rate due to *e-h* pair creation is negligible. The rate rises rapidly with *T* due to the activation energy.

The sharp turn-on and turn-off for $W_{ph}^{\rm res}$ occur near $|K_y^*|\simeq\xi_g^{-1}\equiv nE_g/\hbar{\rm c}$, where the photon has roughly the gap energy. On the other hand, the two peaks for $W_{dp}^{\rm res}$ occur near $|K_y^*|\simeq 1/d$, where the dipolar interaction is most efficient according to Eq. (7). Because $\xi_g\simeq 353$ Å$<d=375$ Å, the two peaks of $W_{dp}^{\rm res}$ are inside of those of $W_{ph}^{\rm res}$ in Figs. 4 and 5.

In summary, we showed that an in-plane *B* quenches the Stokes rate between direct and indirect QWs at low *T*. A higher *B* opens, within a narrow range of *B*, a new fast resonant channel for both the Stokes and anti-Stokes transfer between a higher-energy direct and a lower-energy indirect exciton state. This resonant rate is a few orders of magnitude larger than the $B=0$ rate that arises from creation of *e-h* pairs. The abrupt *B*-dependent turn-on and turn-off behavior of the photon-exchange transfer can be used to identify the radiative transfer mechanism. Low-energy plane-wave states in the indirect QW are essential for the above behavior. However, the excitons may be localized in the direct QW. In this case, the energy-dispersion curve of QW1 in Figs. 2 and 3 is flat, yielding a qualitatively similar behavior.

The resonant transfer discussed here is similar to the *B*-induced interlayer conductance between two electron layers. Here *B* shifts the Fermi circle of one layer relative to that of the other in *k* space. A resonant tunneling current is induced as in Figs. 4 and 5, when the two Fermi circles intersect each other, satisfying simultaneous energy-momentum conservation.[11]

Sandia is a multiprogram laboratory operated by Sandia Corporation, a Lockheed Martin Company, for the U.S. DOE under Contract No. DE-AC04-94AL85000.

[1] T. Takagahara, Phys. Rev. B **31**, 6552 (1985).
[2] A. Tomita, J. Shah, and R.S. Knox, Phys. Rev. B **53**, 10 793 (1996).
[3] D.S. Kim *et al.*, Phys. Rev. B **54**, 14 580 (1996).
[4] S.K. Lyo, Phys. Rev. B **62**, 13 641 (2000).
[5] A. Parlangeli *et al.*, Phys. Rev. B **62**, 15 323 (2000).
[6] Y.J. Chen *et al.*, Phys. Rev. B **36**, 4562 (1987).
[7] C.H. Perry *et al.*, J. Luminescence **48-49**, 725 (1991).
[8] S.K. Lyo, Phys. Rev. B **50**, 4965 (1994).
[9] H. Hasegawa and R.E. Howard, J. Phys. Chem. Solids **21**, 179 (1961); D. Cabib *et al.*, Nuovo Cimento **10**, 185 (1972).
[10] R.L. Greene and K.K. Bajaj, Solid State Commun. **45**, 831 (1983).
[11] J.P. Einstein *et al.*, Phys. Rev. B **44**, 6511 (1991); L. Zheng and A.H. MacDonald, *ibid.*, **47**, 10 619 (1993); S.K. Lyo and J.A. Simmons, J. Phys.: Condens. Matter **5**, L299 (1993).